

# Thermal conductivity of hygroscopic foams based on cellulose nanofibrils and a nonionic polyoxamer

Varvara Apostolopoulou-Kalkavoura · Korneliya Gordeyeva · Nathalie Lavoine · Lennart Bergström

Received: 13 October 2017 / Accepted: 15 December 2017 / Published online: 21 December 2017  
© The Author(s) 2017. This article is an open access publication

**Abstract** Nanocellulose-based lightweight foams are promising alternatives to fossil-based insulation materials for energy-efficient buildings. The properties of cellulose-based materials are strongly influenced by moisture and there is a need to assess and better understand how the thermal conductivity of nanocellulose-based foams depends on the relative humidity and temperature. Here, we report a customized setup for measuring the thermal conductivity of hydrophilic materials under controlled temperature and relative humidity conditions. The thermal conductivity of isotropic foams based on cellulose nanofibrils and a nonionic polyoxamer, and an expanded polystyrene foam was measured over a wide range of temperatures and relative humidity. We show that a previously developed model is unable to capture the strong relative humidity dependence of the thermal conductivity of the hygroscopic, low-density nanocellulose- and nonionic polyoxamer-based foam. Analysis of the moisture uptake and moisture transport was used to develop an empirical model that takes into consideration the moisture content and the wet density of the investigated foam. The new empirical model could predict the thermal conductivity of a foam with a similar composition but almost 3 times higher density.

Accurate measurements of the thermal conductivity at controlled temperature and relative humidity and availability of simple models to better predict the thermal conductivity of hygroscopic, low-density foams are necessary for the development of nanocellulose-based insulation materials.

**Keywords** Thermal conductivity · Nanocellulose · Isotropic foams · Moisture transport · Hygroscopic · Empirical modelling

## List of symbols

$AH$	Absolute humidity
$B$	Moisture supplement
CNF	Cellulose nanofibrils
EPS	Expanded polystyrene
GDL	Gluconic acid d-lactone
$H_2O_{vl}$	Moisture content by volume
$H_2O_w$	Moisture content by mass
$P_w$	Vapor pressure
$P_{ws}$	Saturation pressure
$RH$	Relative humidity
RMSE	Root-mean-square error
SEM	Scanning electron microscopy
TGA	Thermogravimetric analysis
$\gamma(T)$	Temperature-dependent supplement
$\lambda_{dry}$	Thermal conductivity of the dry material
$\lambda_{wet}$	Wet (effective) thermal conductivity
$\rho_{dry}$	Dry density of the foam
$\rho_{wet}$	Wet density of the foam

V. Apostolopoulou-Kalkavoura · K. Gordeyeva · N. Lavoine · L. Bergström (✉)  
Department of Materials and Environmental Chemistry,  
Stockholm University, Stockholm, Sweden  
e-mail: lennart.bergstrom@mmk.su.se

## Introduction

Development of high performance thermally insulating materials from renewable or widely abundant resources could substantially improve the energy efficiency of buildings and reduce the environmental impact (Papadopoulos 2005; Berge and Johansson 2012; IEA 2013). Indeed, the energy consumed to maintain a pleasant interior environment by space heating and cooling accounts for more than 10% of the global energy consumption (IEA 2013).

Biopolymer-based materials such as cork and wood chips were extensively used for thermal insulation prior to the introduction of fossil fuel-based foams, but their insulating performance is relatively poor (Jelle 2011). Nanocellulose features an attractive combination of properties like a high elastic modulus, low thermal expansion coefficient, and tunable surface chemistry (Klemm et al. 2011; Moon et al. 2011; Duong and Nguyen 2016). From nanocellulose gel-like suspension, ultralight weight (density  $\leq 10 \text{ kg/m}^3$ ) and highly porous (porosity  $\geq 99\%$ ) foams can be produced via different techniques such as ice templating (Wicklein et al. 2014; Munier et al. 2016), supercritical drying (Medina-Gonzalez et al. 2012; Lavoine and Bergström 2017) or blending (Gordeyeva et al. 2016). The controlled surface chemistry, interparticle bonding and assembly of nanocellulose can result in nanocellulose foams with a high compressive strength and low thermal conductivity (Lavoine and Bergström 2017).

Cellulose is a hygroscopic material and the properties of cellulose-based materials are well-known to be strongly dependent on the moisture content (Lindström et al. 2012). Studies on cellulosic materials such as paper show that elastic moduli and tensile strength are significantly decreased at high relative humidity conditions (Bandyopadhyay et al. 2000). Composite foams made of amylopectin and nanocellulose also showed a 30% decrease in storage modulus with increasing relative humidity from 20 to 80% (Svagan et al. 2008). Agarwal et al. (Agarwal et al. 2017) reported that the crystallinity index of cellulose pulp decreased with increasing moisture content; highlighting the importance of storing cellulose-based materials at controlled humidity/temperature conditions prior to measurement.

Recent works have shown that nanocellulose foams can display thermal conductivity below 25 mW/mK

(Wicklein et al. 2014; Sakai et al. 2016), which classifies them as superinsulating materials. Depending on the cellulose source and how the foams/aerogels have been produced, the thermal conductivity of nanocellulose foams and aerogels varied between 20 and 40 mW/mK (Jelle 2011; Kobayashi et al. 2014; Sakai et al. 2016; Jimenez-Saelices et al. 2017). To date, however, studies on the thermal conductivity of nanocellulose-based foams and aerogels are sparse and have primarily assessed the thermal conductivity of the porous materials at constant temperature and/or constant relative humidity (Silva et al. 2010; Isogai et al. 2011; Nguyen et al. 2014; Wicklein et al. 2014; Jimenez-Saelices et al. 2017).

We have developed an experimental setup which can perform accurate measurements of the thermal conductivity within a wide range of temperatures ( $-12$  to  $+41 \text{ }^\circ\text{C}$ ) and relative humidity (2–80% RH). The thermal conductivity of a low-density nanocellulose- and nonionic polyoxamer-based foam was determined and compared with that of a low-density polystyrene foam. In parallel, we have also determined the moisture uptake and the moisture transport properties of the foams in order to correlate the heat and moisture transfer in the foams. We establish and discuss an empirical model, which can accurately describe the thermal conductivity of the investigated low-density foams over a wide relative humidity range.

## Materials and methods

### Materials

A never-dried sulfite softwood cellulose pulp (Domsjö dissolving Plus; Aditya Birla Domsjö, Sweden) was kindly provided by the Fiber technology and Polymer division of the Royal Institute of Technology (KTH, Stockholm, Sweden). Sodium hypochlorite (NaClO, Alfa Aesar), 2,2,6,6-tetramethyl-1-piperidinyloxy free radical (TEMPO,  $\geq 98\%$ , Alfa Aesar), sodium hydroxide (NaOH, P99.2%, VWR Chemicals) and sodium bromide (NaBr, BioUltra, P99.5%, Sigma Aldrich) were used as received. Hydrochloric acid (HCl, VWR Chemicals, 35%), pluronic triblock (EO-PO-EO) copolymer P123 ( $M_n = 5750 \text{ g mol}^{-1}$ , BASF Corporation), calcium chloride ( $\text{CaCl}_2$ , minimum 93%, Sigma Aldrich), sodium carbonate ( $\text{Na}_2\text{CO}_3$ , BioXtra, P99%, Sigma Aldrich) and D-(+)-

gluconic acid D-lactone (GDL, P99%, Sigma Aldrich) were used as received in the preparation of the foams.

TEMPO-oxidized cellulose nanofibrils (CNF) were prepared as previously reported using the TEMPO/NaBr/NaClO system with 15 mmol of NaClO per gram of cellulose (Blomfeldt et al. 2012; Budaiwi and Abdou 2013). The TEMPO-mediated oxidation was performed for 3 h, at pH 10. The CNF were then obtained by disintegrating the oxidized pulp by repeatedly passing the dispersion four times through the 400 and 200  $\mu\text{m}$  chambers of a high pressure (1600 bars) Microfluidizer (M-110EH, Microfluidics) (Gordeyeva et al. 2016).

Foams containing CNF, P123,  $\text{CaCO}_3$  and GDL were prepared by mixing a CNF suspension at two different concentrations; 0.5 or 0.7 wt% with the dispersion of  $\text{CaCO}_3$  particles and the triblock poly(ethylene glycol)-poly(propylene glycol)-poly(ethylene glycol) polyoxamer copolymer, P123. The obtained mixture was foamed using a dispersing tool, Ultra-Turrax (T18 IKA Werke, Germany) for 3 min at 7000 rpm with the dropwise addition of GDL performed at the last minute of the foaming (Gordeyeva et al. 2016).

Expanded polystyrene (EPS, Quality S80, Bewi) with a density of  $14.1 \pm 0.9 \text{ kg/m}^3$  was used as a reference material (Bewi Insulation 2016).

#### Characterization of the foams

Scanning electron microscopy (SEM) images of the foam cross-section were taken using a HITACHI TM-3000 (Germany, 5 kV,  $\times 500$ ).

Nitrogen sorption measurements were performed using an ASAP 2020 (Micromeritics Instrument Corporation, Norcross, GA, USA). The BET (Brunauer–Emmett–Teller) and BJH (Barret–Joyner–Halenda) models were used to estimate the surface area and pore volume of the foams, respectively. The CNF foams were degassed at 80 °C for 10 h prior to the measurements.

The charge density of CNF was determined by conductometric titrations and estimated to be  $1603 \pm 5 \mu\text{eq/g}$  (Committee 2002).

The density of the foams was calculated from the mass and the volume of the foams which was measured with a caliper.

The porosity ( $\varepsilon$ ) of the foams was estimated from the composition and the densities of the different components in the foam.

#### Thermal conductivity measurement

The thermal conductivity ( $\lambda$ , mW/mK) of the EPS and CNF- and nonionic polyoxamer-based foams was measured using the TPS 2500 S Hot Disk Thermal Constants Analyzer in isotropic mode. The TPS sensor (3.2 mm in radius) was placed between two identical pieces of EPS (diameter:  $4.1 \pm 0.1 \text{ cm}$ ; height:  $2.2 \pm 0.2 \text{ cm}$ ) or CNF- and nonionic polyoxamer-based foams (diameter:  $4.3 \pm 0.1 \text{ cm}$ ; height:  $1.6 \pm 0.2 \text{ cm}$ ) and thermal contact between the sensor and the foams were ensured by slightly pressing the foam onto the sensor (Gustafsson 1991; Dixon et al. 2000). The heating power was 10 mW and the measurement time was 10 s for each thermal conductivity measurement. The foams were enclosed in a customized cell, allowing the relative humidity ( $RH$ ) to be controlled within the range 2–80%  $RH$  using a P2 Cellkraft humidifier (Ocklind 2016). The temperature of the foams was controlled (261–314 K) by immersing the customized cell in a temperature controlled silicon oil bath. Five independent measurements were performed with 15 min interval time for each temperature and  $RH$  on 3 pairs of the investigated foams. The foams were kept at the set temperature and  $RH$  for at least 120 min prior to measurements of the thermal conductivity.

#### Moisture transport properties

The water vapor sorption of the CNF- and nonionic polyoxamer-based foams under controlled  $RH$  and temperature was determined by measuring the weight change using a high-precision balance (BP 210 S, Sartorius, Germany) placed inside a humidity chamber. Prior to the measurements, the foams were dried at 40 °C and 10%  $RH$ . The moisture content ( $H_2O_w$ ) as a function of  $RH$  (20, 35, 50, 65 and 80%) was assessed at two different temperatures (22 and 40 °C). Each measurement lasted 6 h to ensure that steady state was reached and the foam mass was measured every 5 min. The water vapor permeability (WVP) was determined following the standard E96 method (ASTM International 2002; Bedane et al. 2016). The foam was sealed from all lateral sides by using a cylindrical Teflon beaker. The bottom of the beaker was covered with Si-gel to maintain dry conditions under the foam while the upper part of the foam was exposed to humid environment.

## Results and discussion

Low density, isotropic CNF- and nonionic polyoxamer-based foams were prepared by a previously reported method that involved foaming an aqueous CNF-based dispersion containing a non-ionic polyoxamer copolymer, Pluronic P123, and crosslinking the CNF by calcium ions that were released by a triggered pH decrease using gluconic acid d-lactone (GDL) (Gordeyeva et al. 2016). The wet foams were oven-dried at 60 °C to obtain dry foams with a final composition of 46.3 wt% CNF, 32.4 wt% P123, 4.6 wt%  $\text{CaCO}_3$  and 16.7 wt% GDL (Fig. 1a).

The dry CNF- and nonionic polyoxamer-based foam with a density of  $11.9 \pm 1.2 \text{ kg/m}^3$  and an approximate porosity of 99%, displayed a closed foam macrostructure with an average foam pore diameter of  $145 \pm 46 \text{ }\mu\text{m}$  (Gordeyeva et al. 2016) (Fig. 1b). The specific surface area of the foam was around  $1\text{--}2 \text{ m}^2/\text{g}$ , which suggested that the porosity of the pore wall was low.

The thermal conductivity of the foams at controlled humidity and temperature was assessed in a closed measurement cell with inlet and outlet for the humidified air and apertures for the  $\Delta T$  sensor and the humidity/temperature sensor (Fig. 2). The temperature is controlled by immersing the measurement cell in an oil bath and the relative humidity (*RH*) is controlled using a humidifier. The *RH* represents the ratio between the partial vapor pressure ( $P_w$ ) and the water vapor saturation pressure ( $P_{ws}$ ) (Parish and Putnam 1977).

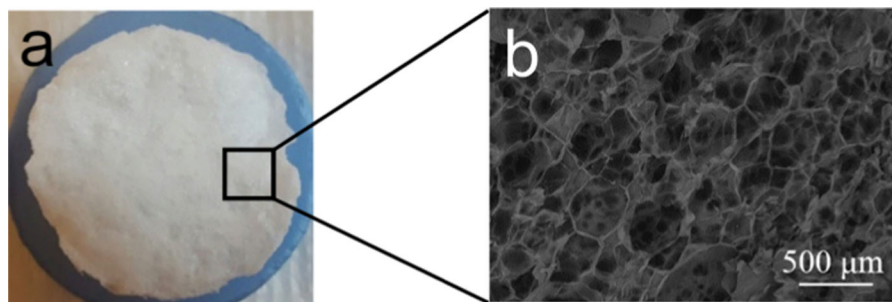
Comparison of the CNF- and nonionic polyoxamer-based foam with a commercial expanded polystyrene (EPS) foam showed that the temperature dependence of the two materials is similar at low humidity (Fig. 3a). The thermal conductivity values measured

for the isotropic CNF- and nonionic polyoxamer-based foam at low humidity ( $1.18 \pm 0.1 \text{ g H}_2\text{O/m}^3$  air, which corresponds to 5% *RH* at 299 K) range between 43 and 48 mW/mK, which correlates well with previous measurements of the thermal conductivity of cellulose and other biopolymer foams (Jelle 2011; Blomfeldt et al. 2012; Lavoine and Bergström 2017).

The thermal conductivity of the EPS foam was found to be identical to the value given by the manufacturer (38 mW/mK), which confirms that the customized setup is able to accurately measure the thermal conductivity.

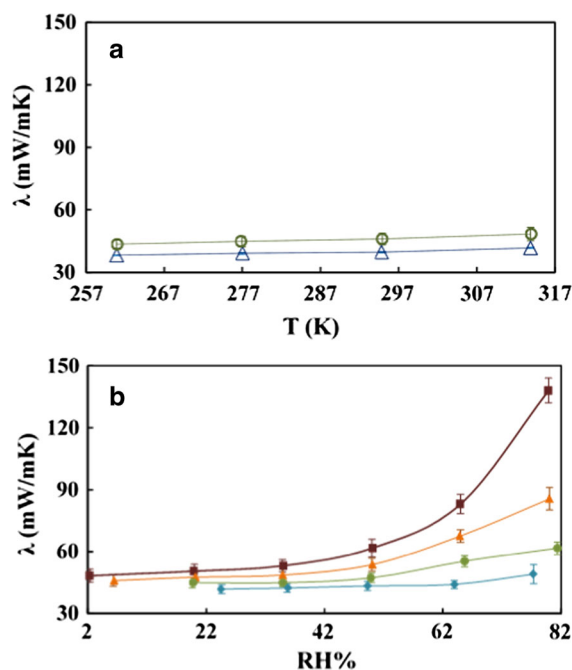
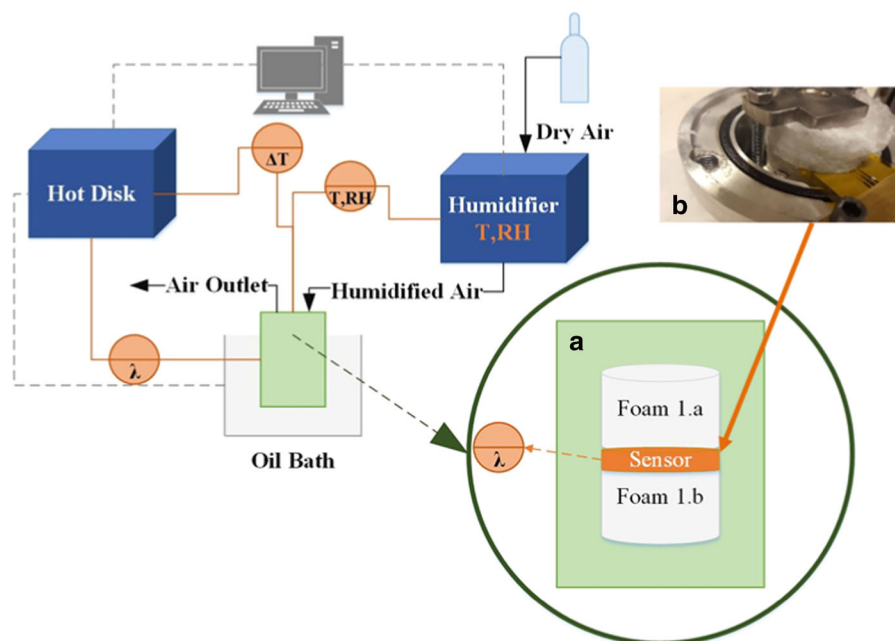
The thermal conductivity of the CNF- and nonionic polyoxamer-based foam at constant humidity increased by 11% when the temperature is increased from 257 to 317 K (Fig. 3a). The linear temperature dependence of the thermal conductivity of the CNF- and nonionic polyoxamer-based foam is similar to other porous and cellular materials such as wood (Jansson 2004), fireboard (Jansson 2004), fiberglass (Abdou and Budaiwi 2013; Budaiwi and Abdou 2013), PMMA (Jansson 2004), expanded glass granules, foam glass gravel (Ochs et al. 2008), polystyrene (Jansson 2004; Algaer 2010) and polyurethane foams (Al-Ajlan 2006; Jarfelt and Ramnäs 2006).

Figure 3b shows that the thermal conductivity of the CNF- and nonionic polyoxamer-based isotropic foam increased significantly with increasing relative humidity. Previous studies have shown that the thermal conductivity of other hygroscopic materials, e.g. wood, concrete, expanded glass granules (Hansen 1993; Künzel 1995; Künzel and Kiessl 1996; Belbekhouche et al. 2011), displayed a similar dependence on the humidity and temperature as observed for the CNF-based foams in this study.



**Fig. 1** CNF- and nonionic polyoxamer-based foam. **a** Picture of the solid foam, **b** SEM image of the porous structure of the foam

**Fig. 2** Experimental setup for thermal conductivity measurements under controlled temperature and relative humidity consisting of a TPS 2500 S Hot Disk Thermal Constants Analyzer and a P2 Cellkraft Humidifier. **a** Enclosed measurement cell, **b** the CNF- and nonionic polyoxamer-based foams and the hot disk sensor inside the measurement cell



**Fig. 3** Thermal conductivity of CNF- and nonionic polyoxamer-based foam. **a** Thermal conductivity ( $\lambda$ ) of CNF- and nonionic polyoxamer-based foams (open circle), and EPS foam (open triangle) as a function of temperature, at constant absolute humidity ( $AH = 1.19 \pm 0.1 \text{ g H}_2\text{O/m}^3 \text{ air}$ ), **b** thermal conductivity ( $\lambda$ ) of CNF- and nonionic polyoxamer-based foams as a function of the relative humidity (RH %) at 314 (filled square), 295 (filled triangle), 277 (filled circle) and 262 K (filled diamond)

Figure 4 shows that the moisture uptake of the CNF- and nonionic polyoxamer-based foam at low RH was significantly lower at 314 than at 295 K; the moisture uptake at 35% RH was e.g.  $6.44 \pm 0.94\%$  at 295 K compared to only  $0.26 \pm 0.16\%$  at 314 K. Hence, at 314 K and 10% RH, the CNF- and nonionic polyoxamer-based foam was almost moisture free. All the foams were therefore conditioned at 10% RH and 314 K prior to the moisture uptake measurements. Other hydrophilic polysaccharides, such as chitosan (Aguirre-loredo et al. 2017), starch (Al-Muhtaseb et al. 2004), and potato (Wang 1991) also display a

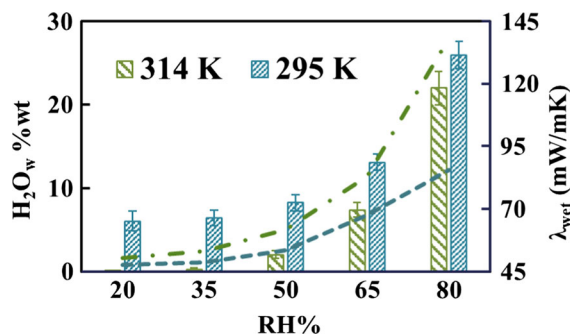


**Fig. 4** Moisture content,  $\text{H}_2\text{O}_w$  (wt%) (histogram) and thermal conductivity of the CNF- and nonionic polyoxamer-based foam as a function of the relative humidity (RH %) at 314 (continuous line) and 295 K (dashed line)



similar decrease of the moisture content with increasing temperature.

Ochs et al. (2008) suggested that the thermal conductivity of hygroscopic insulation materials is related to the replacement of air by water in the pores. The thermal conductivity of water (580 mW/mK) is more than 20 times higher than the conductivity of dry air (25 mW/mK); hence, even a small increase of the moisture content is expected to result in a significant increase in the thermal conductivity of hygroscopic materials.

The thermal conductivity of hygroscopic (building) materials has previously been described by Künzle et al. (Künzel 1995) using Eq. 1:

$$\lambda_{wet} = \lambda_{dry} * \left( 1 + \frac{b * H_2O_{vl}}{\rho_{dry}} \right) \quad (1)$$

where,  $\lambda_{dry}$  is the thermal conductivity of the dry foam,  $b$  is the dimensionless moisture supplement,  $H_2O_{vl}$  is the moisture content by volume ( $\text{kg/m}^3$ ) of the foam, and  $\rho_{dry}$  is the dry density of the foam. The Künzle model relies on the hypothesis that the wet thermal conductivity of insulation materials,  $\lambda_{wet}$ , is a linear function of the materials' volumetric water content ( $H_2O_{vl}$ ). Indeed, Künzle et al. (Künzel 1995; Künzel and Kiessl 1996) showed that this requirement is met for insulation materials such as wood, normal concrete, expanded clay concrete and silica brick (Künzel 1995; Künzel and Kiessl 1996).

Figure 5a shows that the Künzle model significantly underestimates the strong dependence on

relative humidity of the thermal conductivity of the hygroscopic CNF- and nonionic polyoxamer-based foam. Figure 5b shows, indeed, that the relationship between the (wet) thermal conductivity and the moisture content by volume of the CNF- and nonionic polyoxamer-based foams is not linear, confirming that the Künzle model is unsuitable to describe the thermal conductivity of the investigated CNF- and nonionic polyoxamer-based foam. We used a value for  $b$  of 1.5 that previously was used to describe the moisture dependence of the thermal conductivity of wood (Künzel 1995; Künzel and Kiessl 1996). Decreasing or increasing the  $b$  (0.5–5) does not improve the fit to the Künzle model.

Previous works have shown that the moisture transport properties can have a significant influence on the thermal transport properties of hygroscopic foams (Ochs et al. 2008; Künzel 1995; Haghi 2011; Osanyintola and Simonson 2006; Talukdar et al. 2007). The moisture transport properties of the CNF- and nonionic polyoxamer-based foam have been characterized by determining the water vapor permeability,  $WVP$ , and the water vapor resistance factor,  $\mu$ , from the time-dependent mass gain,  $S$ , according to Eq. 2 (ASTM International 2002; Richter and Stan 2016):

$$WVP = \frac{S \times h}{A \times \Delta P}; \quad \mu = \frac{\delta_{air}}{WVP} \quad (2)$$

where,  $S$  is the slope of the mass gain of the foam in g/s,  $h$  is the height of the foam in m,  $A$  is the surface area exposed to the moisture flow in  $\text{m}^2$ ,  $\Delta P$  is the

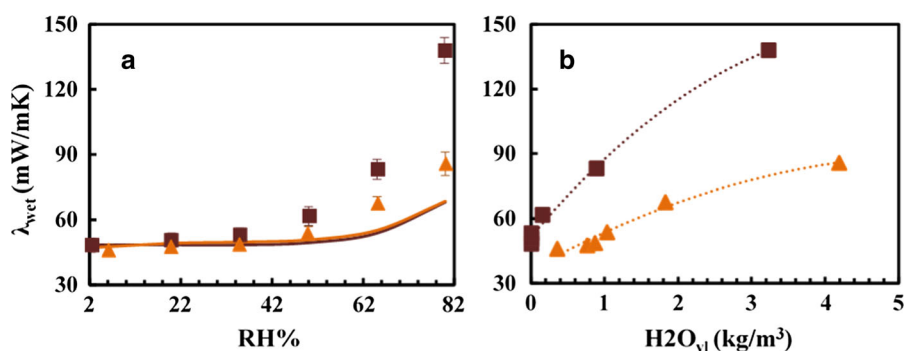


**Fig. 5** Fitting of the experimental data using Künzle's model (Künzel 1995; Künzel and Kiessl 1996). **a** Plot of the thermal conductivity values ( $\lambda$ ) of CNF- and nonionic polyoxamer-based foam calculated by the equation proposed by Künzle et al. (Künzel 1995; Künzel and Kiessl 1996) and plot of the

experimental thermal conductivity values ( $\lambda$ ) of CNF- and nonionic polyoxamer-based foam at 314 K (filled rectangle) and 295 K (filled triangle) as a function of the relative humidity (RH %), **b** experimental thermal conductivity as a function of moisture content by volume

vapor pressure difference between the top and the bottom of the foam in Pa, and  $\delta_{\text{air}}$  is the water vapor diffusion coefficient in air (g/msPa).

Table 1 shows that the water vapor resistance factor of the CNF- and nonionic polyoxamer-based foam ranged between 0.1 and 0.2 at 295 K and between 0.3 and 1 at 314 K, which is much lower than the water vapor resistance factor of hygroscopic materials like concrete, wood, clay brick and silica brick that were the basis for K nzel model (K nzel 1995; K nzel and Kiessl 1996). We speculate that the water vapor permeability has a stronger influence on the thermal conductivity of the CNF- and nonionic polyoxamer-based foam than on the thermal conductivity of the previously investigated materials that displayed much higher water vapor resistance factors (between 7 and 260 (K nzel 1995; K nzel and Kiessl 1996)).

We have made an attempt to introduce a model that accommodates the significant influence of the

moisture content and water vapor permeability on the wet thermal conductivity of the foams.

We find that the  $\lambda_{\text{wet}}$  of the CNF- and nonionic polyoxamer-based foam displayed a linear correlation with the moisture content by mass ( $H_2O_w$ ) (Fig. 6a). It should be noted that the moisture content by mass is the moisture content by volume ( $H_2O_v$ ) divided by the wet density. This seemingly small modification of the K nzel model is related to the difference in density between the insulating materials that the K nzel model was based on and the low-density foams investigated in this study.

The materials investigated by K nzel et al. (1995) all displayed a relatively high density (300–1800 kg/m<sup>3</sup>) and the relative weight increase by moisture uptake was always small. In the present study, however, the density of the CNF- and nonionic polyoxamer-based foam was very low (11.9 kg/m<sup>3</sup>)

**Table 1** Moisture content,  $H_2O_w$ , (wt%), water vapor permeability WVP and water vapor resistance factor,  $\mu$ , of the CNF- and nonionic polyoxamer-based foam as a function of relative humidity (RH) and temperature

RH%	$H_2O_w$ (wt%)		WVP (g/msPa) $\times 10^{-9}$		$\mu$	
	295 K	314 K	295 K	314 K	295 K	314 K
20	6.07	0.03	1.76	0.22	0.11	0.92
35	6.44	0.26	1.13	0.35	0.17	0.59
50	8.5	2.05	1.09	0.44	0.18	0.47
65	13.05	7.41	1.03	0.77	0.19	0.27
80	25.95	21.96	1.24	0.78	0.16	0.27

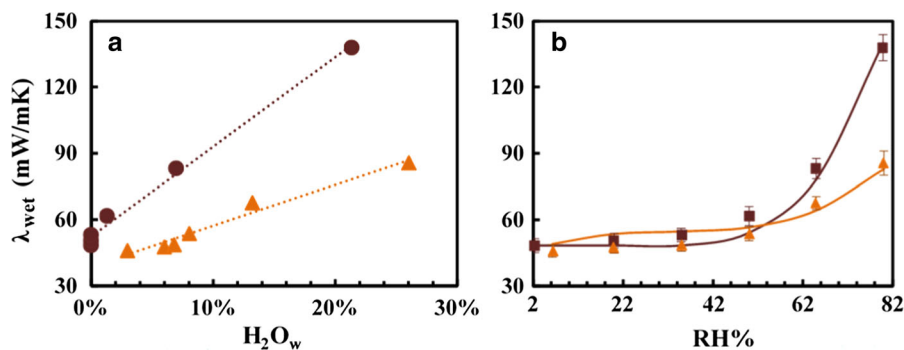


**Fig. 6** Empirical modeling of the experimental thermal conductivity data. **a** Experimental thermal conductivity as a function of moisture content by total mass, **b** plot of the thermal conductivity ( $\lambda_{\text{wet}}$ ) of CNF- and nonionic polyoxamer-based

foam calculated by Eq. 3 (continuous line) and plot of the experimental thermal conductivity ( $\lambda_{\text{wet}}$ ) of CNF- and nonionic polyoxamer-based foam as a function of the relative humidity (RH %) at 314 (filled rectangle) and 295 K (filled triangle)

and the amount of absorbed moisture was as high as the dry mass of the foams.

The modified K nzel model (Eq. 3):

$$\lambda_{\text{wet}} = \lambda_{\text{dry}} \times \left( 1 + \gamma(T) \times \frac{H_2O_{vl}}{\rho_{\text{dry}} + H_2O_{vl}} \right) \quad (3)$$

is based on the wet density of the foam,  $\rho_{\text{wet}} = \rho_{\text{dry}} + H_2O_{vl}$ , and a temperature-dependent supplement,  $\gamma(T)$ . Figure 6b shows that the modified model (Eq. 3) was able to accurately describe the experimental thermal conductivity of the wet CNF- and nonionic polyoxamer-based foam over the entire investigated range of relative humidity. The small RMSE in Table 2 confirms that the modified model provides a good fit to the data.

To validate our model, we attempted to fit Eq. 3 to the thermal conductivity of a CNF- and nonionic polyoxamer-based foam of identical composition but with a higher density (dry density: 28.8 kg/m<sup>3</sup>) than that of the previously investigated foam (dry density of 11.9 kg/m<sup>3</sup>). Figure 7 illustrates that the model is able to accurately describe the relative humidity dependence of the CNF- and nonionic polyoxamer-based foam with the higher density. It should be noted that we used the parameters for  $\gamma(T)$  obtained from the lower density foams and simply assumed that the water uptake scales with the density of the foam. We find that the RMSE for the higher density foam are of similar magnitude as for the lower density foam (Table 2), which suggests that the new empirical model (Eq. 3) is able to describe the thermal conductivity for hygroscopic CNF- and nonionic polyoxamer-based foams of densities within the range 10–30 kg/m<sup>3</sup>. Future work should investigate the general validity of the empirical model by investigating other low-density, hygroscopic foams.

**Table 2** Root-mean-square error (RMSE) of the fit using Eq. 3 for the 11.9 and 28.8 kg/m<sup>3</sup> CNF- and nonionic polyoxamer-based foam, and the related temperature-dependent supplement  $\gamma(T)$

$T$ (K)	RMSE (mW/mK)		$\gamma$ (T)
	$\rho = 11.9 \text{ kg/m}^3$	$\rho = 28.8 \text{ kg/m}^3$	
314 K	0.03–1.93	0.42–1.20	8.86
295 K	0.29–1.85	0.75–1.84	3.26

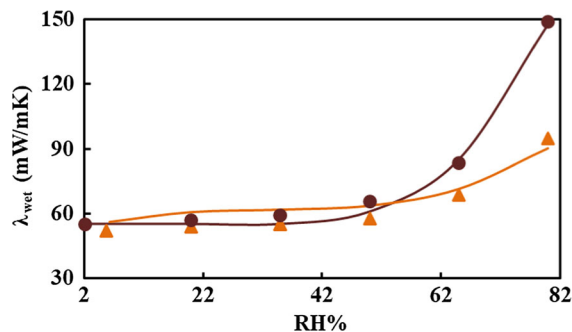


**Fig. 7** Plot of the thermal conductivity ( $\lambda$ ) of the 28.8 kg/m<sup>3</sup> CNF- and nonionic polyoxamer-based foams calculated by Eq. 3 (continuous line) and plot of the experimental thermal conductivity ( $\lambda_{\text{wet}}$ ) of the 28.8 kg/m<sup>3</sup> CNF- and nonionic polyoxamer-based foams as a function of the relative humidity (RH %) at 314 (filled rectangle) and 295 K (filled triangle)

## Conclusion

Measurements of the thermal conductivity at controlled temperature and humidity of hygroscopic cellulose nanofibril- and nonionic polyoxamer-based foams have been performed using a customized measurement cell in a hot disk device. The thermal conductivity of isotropic CNF- and nonionic polyoxamer-based foams increased more than 3 times as the temperature and relative humidity increased from 261 K and 2% RH, to 314 K and 80% RH. We showed that both the moisture uptake and the moisture transport properties have a significant influence on the thermal conductivity of the CNF- and nonionic polyoxamer-based foams.

K nzel's model was unable to accurately describe the thermal conductivity of the hygroscopic, low-density CNF and nonionic polyoxamer-based foams. We have developed an empirical model based on the linear relation between  $\lambda_{\text{wet}}$  of the CNF and nonionic polyoxamer-based foams with the moisture content by mass that was able to describe the thermal conductivity of the CNF and nonionic polyoxamer-based foams over the entire RH-range. Analysis of the moisture uptake and moisture transport properties suggests that K nzel's model is valid for materials with relatively high densities and (very) high water vapor resistance factors ( $\mu \geq 7$ ), while the new empirical model is valid for foams with low densities and low water vapor resistance factors ( $\mu \leq 1$ ). Combining accurate measurements of thermal conductivity at controlled temperatures and relative humidity with the empirical



model developed in this study paves the way for predicting the thermal performances of hygroscopic, low-density foams.

**Acknowledgments** We would like to acknowledge the Swedish Energy Agency (Energimyndigheten) and the Swedish Foundation for strategic research (SSF) for funding this project. We also thank Andreas Fall for technical support on the cell design and Daniela Stoeckel for valuable suggestions.

**Open Access** This article is distributed under the terms of the Creative Commons Attribution 4.0 International License (<http://creativecommons.org/licenses/by/4.0/>), which permits unrestricted use, distribution, and reproduction in any medium, provided you give appropriate credit to the original author(s) and the source, provide a link to the Creative Commons license, and indicate if changes were made.

## References

- Abdou A, Budaiwi I (2013) The variation of thermal conductivity of fibrous insulation materials under different levels of moisture content. *Constr Build Mater* 43:533–544. <https://doi.org/10.1016/j.conbuildmat.2013.02.058>
- Agarwal UP, Ralph SA, Baez C et al (2017) Effect of sample moisture content on XRD-estimated cellulose crystallinity index and crystallite size. *Cellulose* 24:1971–1984. <https://doi.org/10.1007/s10570-017-1259-0>
- Aguirre-loredo RY, Rodriguez-hernandez AI, Velazquez G (2017) Modelling the effect of temperature on the water sorption isotherms of chitosan films. *Food Sci Technol* 37:112–118
- Al-Ajlan SA (2006) Measurements of thermal properties of insulation materials by using transient plane source technique. *Appl Therm Eng* 26:2184–2191. <https://doi.org/10.1016/j.applthermaleng.2006.04.006>
- Algaer E (2010) Thermal conductivity of polymer materials reverse nonequilibrium molecular dynamics simulation. Technische Universität Darmstadt
- Al-Muhtaseb AH, McMinn WAM, Magee TRA (2004) Water sorption isotherms of starch powders: Part 1: mathematical description of experimental data. *J Food Eng* 61:297–307. [https://doi.org/10.1016/S0260-8774\(03\)00133-X](https://doi.org/10.1016/S0260-8774(03)00133-X)
- ASTM International (2002) Standard test methods for water vapor transmission of materials 1. *ASTM Int* i:1–10
- Bandyopadhyay A, Radhakrishnan H, Ramarao BV, Chatterjee SG (2000) Moisture sorption response of paper subjected to ramp humidity changes: modeling and experiments. *Ind Eng Chem Res* 39:219–226. <https://doi.org/10.1021/ie990279w>
- Bedane AH, Eic M, Farmahini-Farahani M, Xiao H (2016) Theoretical modeling of water vapor transport in cellulose-based materials. *Cellulose* 23:1537–1552. <https://doi.org/10.1007/s10570-016-0917-y>
- Belbekhouche S, Bras J, Siqueira G et al (2011) Water sorption behavior and gas barrier properties of cellulose whiskers and microfibrils films. *Carbohydr Polym* 83:1740–1748. <https://doi.org/10.1016/j.carbpol.2010.10.036>
- Berge A, Johansson P (2012) Literature review of high performance thermal insulation. Gothenburg, Chalmers University of Technology
- Bewi Insulation (2016) BEWI EPS STANDARD. <http://www.bewiinsulation.com/se/pdf/EPS-STANDARD.pdf>
- Blomfeldt TOJ, Nilsson F, Holgate T et al (2012) Thermal conductivity and combustion properties of wheat gluten foams. *ACS Appl Mater Interfaces* 4:1629–1635. <https://doi.org/10.1021/am2017877>
- Budaiwi I, Abdou A (2013) The impact of thermal conductivity change of moist fibrous insulation on energy performance of buildings under hot-humid conditions. *Energy Build* 60:388–399. <https://doi.org/10.1016/j.enbuild.2013.01.035>
- Committee S pulp paper and board testing (2002) Total acidic group content. Scandinavian pulp, paper and board testing committee, pp 1–4
- Dixon C, Strong MR, Zhang SM (2000) Transient plane source technique for measuring thermal properties of silicone materials used in electronic assemblies. *Int J Microcircuits Electron Packag* 23:494–500
- Duong HM, Nguyen ST (2016) Nanocellulose aerogels as thermal insulation materials. In: Pacheco TF, Buratti C, Kalaiselvam S, Granqvist CG, Ivanov V (eds) *Nano and biotech based materials for energy building efficiency*. Springer, Cham
- Gordeyeva KS, Fall AB, Hall S et al (2016) Stabilizing nanocellulose-nonionic surfactant composite foams by delayed Ca-induced gelation. *J Colloid Interface Sci* 472:44–51. <https://doi.org/10.1016/j.jcis.2016.03.031>
- Gustafsson SE (1991) Transient plane source techniques for thermal conductivity and thermal diffusivity measurements of solid materials. *Rev Sci Instrum* 62:797–804. <https://doi.org/10.1063/1.1142087>
- Haghi AK (2011) Heat & mass transfer in textiles. WSEAS Press, Montreal
- Hansen MH (1993) Estimation of transfer coefficients in models for coupled heat and moisture transfer in porous media. Building Materials Laboratory, Technical University of Denmark
- International Energy Agency (2013) Transition to sustainable buildings: strategies and opportunities to 2050
- Isogai A, Saito T, Fukuzumi H (2011) TEMPO-oxidized cellulose nanofibers. *Nanoscale* 3:71–85. <https://doi.org/10.1039/c0nr00583e>
- Jansson R (2004) Measurement of thermal properties at elevated temperatures-brandforsk project 328-031
- Jarfelt U, Ramnäs O (2006) Thermal conductivity of polyurethane foam—best performance thermal conductivity of polyurethane foam best performance. In: 10th international symposium on district heating and cooling. Göteborg, p 12
- Jelle BP (2011) Traditional, state-of-the-art and future thermal building insulation materials and solutions—properties, requirements and possibilities. *Energy Build* 43:2549–2563. <https://doi.org/10.1016/j.enbuild.2011.05.015>
- Jimenez-Saelices C, Seantier B, Cathala B, Grohens Y (2017) Spray freeze-dried nanofibrillated cellulose aerogels with thermal superinsulating properties. *Carbohydr Polym*

- 157:105–113. <https://doi.org/10.1016/j.carbpol.2016.09.068>
- Klemm D, Kramer F, Moritz S et al (2011) Nanocelluloses: a new family of nature-based materials. *Angew Chemie—Int Ed* 50:5438–5466. <https://doi.org/10.1002/anie.201001273>
- Kobayashi Y, Saito T, Isogai A (2014) Aerogels with 3D ordered nanofiber skeletons of liquid-crystalline nanocellulose derivatives as tough and transparent insulators. *Angew Chem Int Ed Engl* 53:10394–10397. <https://doi.org/10.1002/anie.201405123>
- Künzel HM (1995) Simultaneous heat and moisture transport in building components one- and two-dimensional calculation using simple parameters. Fraunhofer Institute of Building Physics, Stuttgart
- Künzel HM, Kiessl K (1996) Calculation of heat and moisture transfer in exposed building components. *Int J Heat Mass Transf* 40:159–167
- Lavoine N, Bergström L (2017) Nanocellulose-based foams and aerogels: processing, properties, and applications. *J Mater Chem A*. <https://doi.org/10.1039/c7ta02807e>
- Lindström SB, Karabulut E, Kulachenko A et al (2012) Mechanosorptive creep in nanocellulose materials. *Cellulose* 19:809–819. <https://doi.org/10.1007/s10570-012-9665-9>
- Medina-Gonzalez Y, Camy S, Condoret J-S (2012) Cellulosic materials as biopolymers and supercritical CO<sub>2</sub> as a green process: chemistry and applications. *Int J Sustain Eng* 5:47–65. <https://doi.org/10.1080/19397038.2011.613488>
- Moon RJ, Martini A, Nairn J et al (2011) Cellulose nanomaterials review: structure, properties and nanocomposites. *Chem Soc Rev* 40:3941–3994. <https://doi.org/10.1039/c0cs00108b>
- Munier P, Gordeyeva K, Bergström L, Fall AB (2016) Directional freezing of nanocellulose dispersions aligns the rod-like particles and produces low-density and robust particle networks. *Biomacromol* 17:1875–1881. <https://doi.org/10.1021/acs.biomac.6b00304>
- Nguyen ST, Feng J, Ng SK et al (2014) Advanced thermal insulation and absorption properties of recycled cellulose aerogels. *Colloids Surfaces A Physicochem Eng Asp* 445:128–134. <https://doi.org/10.1016/j.colsurfa.2014.01.015>
- Ochs F, Heidemann W, Müller-Steinhagen H (2008) Effective thermal conductivity of moistened insulation materials as a function of temperature. *Int J Heat Mass Transf* 51:539–552. <https://doi.org/10.1016/j.ijheatmasstransfer.2007.05.005>
- Ocklind A (2016) Humidifier P-series. In: Cellkraft. <http://www.cellkraft.se/downloads/P-Series.pdf>
- Osanyintola OF, Simonson CJ (2006) Moisture buffering capacity of hygroscopic building materials: experimental facilities and energy impact. *Energy Build* 38:1270–1282. <https://doi.org/10.1016/j.enbuild.2006.03.026>
- Papadopoulos AM (2005) State of the art in thermal insulation materials and aims for future developments. *Energy Build* 37:77–86. <https://doi.org/10.1016/j.enbuild.2004.05.006>
- Parish OO, Putnam TW (1977) Equations for the determination of humidity from dewpoint and psychrometric data. Nasa, Washington, DC
- Richter J, Stan K (2016) Measurements of water vapour permeability—tightness of fibreglass cups and different sealants and comparison of  $\mu$ -value of gypsum plaster boards. *Procedia Eng* 151:277–283. <https://doi.org/10.1016/j.proeng.2016.07.377>
- Sakai K, Kobayashi Y, Saito T, Isogai A (2016) Partitioned airs at microscale and nanoscale: thermal diffusivity in ultra-high porosity solids of nanocellulose. *Sci Rep* 6:20434. <https://doi.org/10.1038/srep20434>
- Silva MC, Takahashi JA, Chaussy D et al (2010) Composites of rigid polyurethane foam and cellulose fiber residue. *J Appl Polym Sci* 117:3665–3672
- Svagan BAJ, Samir MASA, Berglund LA (2008) Biomimetic foams of high mechanical performance based on nanostructured cell walls reinforced by native cellulose nanofibrils. *Adv Mater* 20:1263–1269. <https://doi.org/10.1002/adma.200701215>
- Talukdar P, Olutmayin SO, Osanyintola OF, Simonson CJ (2007) An experimental data set for benchmarking 1-D, transient heat and moisture transfer models of hygroscopic building materials. Part I: experimental facility and material property data. *Int J Heat Mass Transf* 50:4527–4539. <https://doi.org/10.1016/j.ijheatmasstransfer.2007.03.026>
- Wang N, Brennan JG (1991) Moisture sorption isotherm characteristics of potatoes at four temperatures. *J Food Eng* 14:269–287
- Wicklein B, Kocjan A, Salazar-Alvarez G et al (2014) Thermally insulating and fire-retardant lightweight anisotropic foams based on nanocellulose and graphene oxide. *Nat Nanotechnol* 10:277–283. <https://doi.org/10.1038/nnano.2014.248>